blood®
Regular Article

TRANSPLANTATION

NK cell recovery after haploidentical HSCT with posttransplant cyclophosphamide: dynamics and clinical implications

Antonio Russo,[1,2,*] Giacomo Oliveira,[1,3,*] Sofia Berglund,[4] Raffaella Greco,[2] Valentina Gambacorta,[1] Nicoletta Cieri,[3] Cristina Toffalori,[1] Laura Zito,[1] Francesca Lorentino,[2] Simona Piemontese,[2] Mara Morelli,[2] Fabio Giglio,[2] Andrea Assanelli,[2] Maria Teresa Lupo Stanghellini,[2] Chiara Bonini,[3,5] Jacopo Peccatori,[2] Fabio Ciceri,[2,5] Leo Luznik,[4,†] and Luca Vago[1,2,†]

[1]Unit of Immunogenetics, Leukemia Genomics and Immunobiology, [2]Hematology and Bone Marrow Transplantation Unit, and [3]Experimental Hematology Unit, Istituto di Ricovero e Cura a Carattere Scientifico San Raffaele Scientific Institute, Milan, Italy; [4]Sidney Kimmel Comprehensive Cancer Center, Johns Hopkins University School of Medicine, Baltimore, MD; and [5]Vita-Salute San Raffaele University, Milan, Italy

KEY POINTS

- **Posttransplantation cyclophosphamide eliminates most mature donor NK cells infused with the graft, including alloreactive NK cells.**
- **High levels of serum interleukin-15 early after HSCT provide a favorable environment for adoptive infusion of mature donor NK cells.**

The use of posttransplant cyclophosphamide (PT-Cy) as graft-versus-host disease (GVHD) prophylaxis has revolutionized haploidentical hematopoietic stem cell transplantation (HSCT), allowing safe infusion of unmanipulated T cell–replete grafts. PT-Cy selectively eliminates proliferating alloreactive T cells, but whether and how it affects natural killer (NK) cells and their alloreactivity is largely unknown. Here we characterized NK cell dynamics in 17 patients who received unmanipulated haploidentical grafts, containing high numbers of mature NK cells, according to PT-Cy–based protocols in 2 independent centers. In both series, we documented robust proliferation of donor-derived NK cells immediately after HSCT. After infusion of Cy, a marked reduction of proliferating NK cells was evident, suggesting selective purging of dividing cells. Supporting this hypothesis, proliferating NK cells did not express aldehyde dehydrogenase and were killed by Cy in vitro. After ablation of mature NK cells, starting from day 15 after HSCT and favored by the high levels of interleukin-15 present in patients' sera, immature NK cells (CD62L$^+$NKG2A$^+$KIR$^-$) became highly prevalent, possibly directly stemming from infused hematopoietic stem cells. Importantly, also putatively alloreactive single KIR$^+$ NK cells were eliminated by PT-Cy and were thus decreased in numbers and antileukemic potential at day 30 after HSCT. As a consequence, in an extended series of 99 haplo-HSCT with PT-Cy, we found no significant difference in progression-free survival between patients with or without predicted NK alloreactivity (42% vs 52% at 1 year, P = NS). Our data suggest that the majority of mature NK cells infused with unmanipulated grafts are lost upon PT-Cy administration, blunting NK cell alloreactivity in this transplantation setting. (*Blood*. 2018;131(2):247-262)

Introduction

Conceiving strategies to render allogeneic hematopoietic stem cell (HSC) transplantation (HSCT) from HLA-haploidentical family donors safe and feasible has been one of the most challenging efforts faced by the HSCT community over the past several decades. Besides having cured numerous patients that lacked a suitable donor, haploidentical HSCT provided fascinating scientific insights into how the immune system operate upon transfer into an allogeneic environment.[1,2]

One the most remarkable discoveries that originated from early trials of haploidentical HSCT was the description of the principles according to which natural killer (NK) cell alloreactivity ensues, and the observation that, when unleashed, it is accompanied by beneficial effects on HSCT outcome, including protection from relapse.[3-5]

In more recent years, another game-changing discovery stemming from haploidentical HSCT has been the demonstration that high-dose posttransplant cyclophosphamide (PT-Cy) can selectively eliminate the most alloreactive donor T-cell clones in vivo.[6-8] This fostered a true revolution in the field, and haploidentical HSCT platforms based on PT-Cy are increasingly being used worldwide,[9,10] not only because of the impressive abatement of graft-versus-host disease (GVHD) incidence they can convey, but also of their very limited requirements in terms of graft processing and specific expertise from the transplant team. It is largely unknown, however, whether the models that were developed in T cell–depleted haploidentical HSCT still hold true in this setting.

The aim of this study is to trace the dynamics of posttransplantation NK cell recovery in 2 independent series of patients who received

Table 1. Characteristics of patients analyzed longitudinally during the posttransplantation follow-up

UPN	Sex	Age (y)	Diagnosis	Refined DFI*	Conditioning regimen†	GVHD prophylaxis‡	Predicted NK alloreactivity§	Graft source	$CD3^+$ cells infused/kg × 10^6	NK cells infused/kg × 10^6
OSR 1	M	33	sAML	Low	Thio-Treo-Flu	PT-Cy-sirolimus-MMF	Yes (C1)	PB	135.28	19.9
OSR 2	M	69	sAML	High	Thio-Treo-Flu‖	PT-Cy-sirolimus-MMF	No	PB	250	17.32
OSR 3	F	24	HL	High	Thio-Treo-Flu	PT-Cy-sirolimus-MMF	No	PB	194.3	9.18
OSR 4	F	62	AML	High	Thio-Treo-Flu	PT-Cy-sirolimus-MMF	Yes (C1)	PB	267.89	17.13
OSR 5	M	57	sAML	Intermediate	Thio-Treo-Flu	PT-Cy-sirolimus-MMF	Yes (C1)	PB	174.91	21.09
OSR 6	F	45	AML	High	Thio-Treo-Flu	PT-Cy-sirolimus-MMF	No	BM	31.55	1.66
OSR 7	M	34	NHL	Very high	Thio-Treo-Flu	PT-Cy-sirolimus-MMF	No	PB	81.9	13.09
OSR 8	F	76	MDS	High	Thio-Treo-Flu‖	PT-Cy-sirolimus-MMF	No	PB	326.4	17.2
OSR 9	M	63	AML	High	Thio-Treo-Flu	PT-Cy-sirolimus-MMF	Yes (Bw4)	PB	98.57	8.02
OSR 10	F	65	AML	High	Thio-Treo-Flu	PT-Cy-sirolimus-MMF	Yes (C2)	PB	98.86	16.58
JHU 1	M	27	AML	High	Flu-CTX-TBI 2 Gy	PT-Cy-tacrolimus-MMF	Yes (C2)	BM	85.5	8.2
JHU 2	M	67	CML	High	Flu-CTX-TBI 2 Gy	PT-Cy-tacrolimus-MMF	No	BM	157.6	5.3
JHU 3	M	56	NHL	Very high	Flu-CTX-TBI 2 Gy	PT-Cy-tacrolimus-MMF	No	BM	73.3	6.3
JHU 4	M	58	sAML	Very high	Flu-CTX-TBI 2 Gy	PT-Cy-tacrolimus-MMF	Yes (C1)	BM	199.2	26.2
JHU 5	M	69	AML	Very high	Flu-CTX-TBI 2 Gy	PT-Cy-tacrolimus-MMF	Yes (C2)	BM	42.5	2.95
JHU 6	M	33	ALL	High	Flu-CTX-TBI 2 Gy	PT-Cy-sirolimus-MMF	No	BM	41.9	5.50
JHU 7	M	65	AML	High	Flu-CTX-TBI 2 Gy	PT-Cy-tacrolimus-MMF	Yes (Bw4)	BM	72.0	6.83

ALL, acute lymphoid leukemia; AML, acute myeloid leukemia; Bw4, HLA-Bw4; C1, HLA-C group 1; C2, HLA-C group 2; CML, chronic myeloid leukemia; DRI, Disease Risk Index; F, female; HL, Hodgkin lymphoma; M, male; MDS, myelodysplastic syndrome; NHL, non-Hodgkin lymphoma; sAML, secondary acute myeloid leukemia.

*DRI calculated according to Armand et al.[49]

†Conditioning regimens: Flu-CTX-TBI 2 Gy, fludarabine (30 mg/m^2/d on days −6 to −2), cyclophosphamide (14.5 mg/kg/d on days −6 and −5), and 200 cGy of TBI on day −1; Thio-Treo-Flu, thiotepa (5 mg/kg/d on days −3 and −2), treosulfan (14 g/m^2/d on days −6 to −4), and fludarabine (30 mg/m^2/d on days −6 to −2).

‡GVHD prophylaxis: PT-Cy-sirolimus-MMF, cyclophosphamide (50 mg/kg) on days +3 and +4, sirolimus (monitored to maintain a target therapeutic plasma level of 5-15 ng/mL) from day +5, mycophenolate mofetil (10 mg/kg 3 times daily) from day 5; PT-Cy-tacrolimus-MMF, cyclophosphamide (50 mg/kg) on days +3 and +4, tacrolimus (monitored to maintain a target therapeutic plasma level of 5-15 ng/mL) from day +5, and mycophenolate mofetil (15 mg/kg twice daily) from day 5.

§Predicted NK alloreactivity: exclusively in the graft-versus-leukemia reaction, calculated according to the Perugia algorithm as the absence in the patient of killer cell immunoglobulin-like receptor ligands (either Bw4, C1, or C2) present in the donor.

‖These patients received a reduced dose of thiotepa (3 mg/kg) and treosulfan (12 gram/m^2) because of old age.

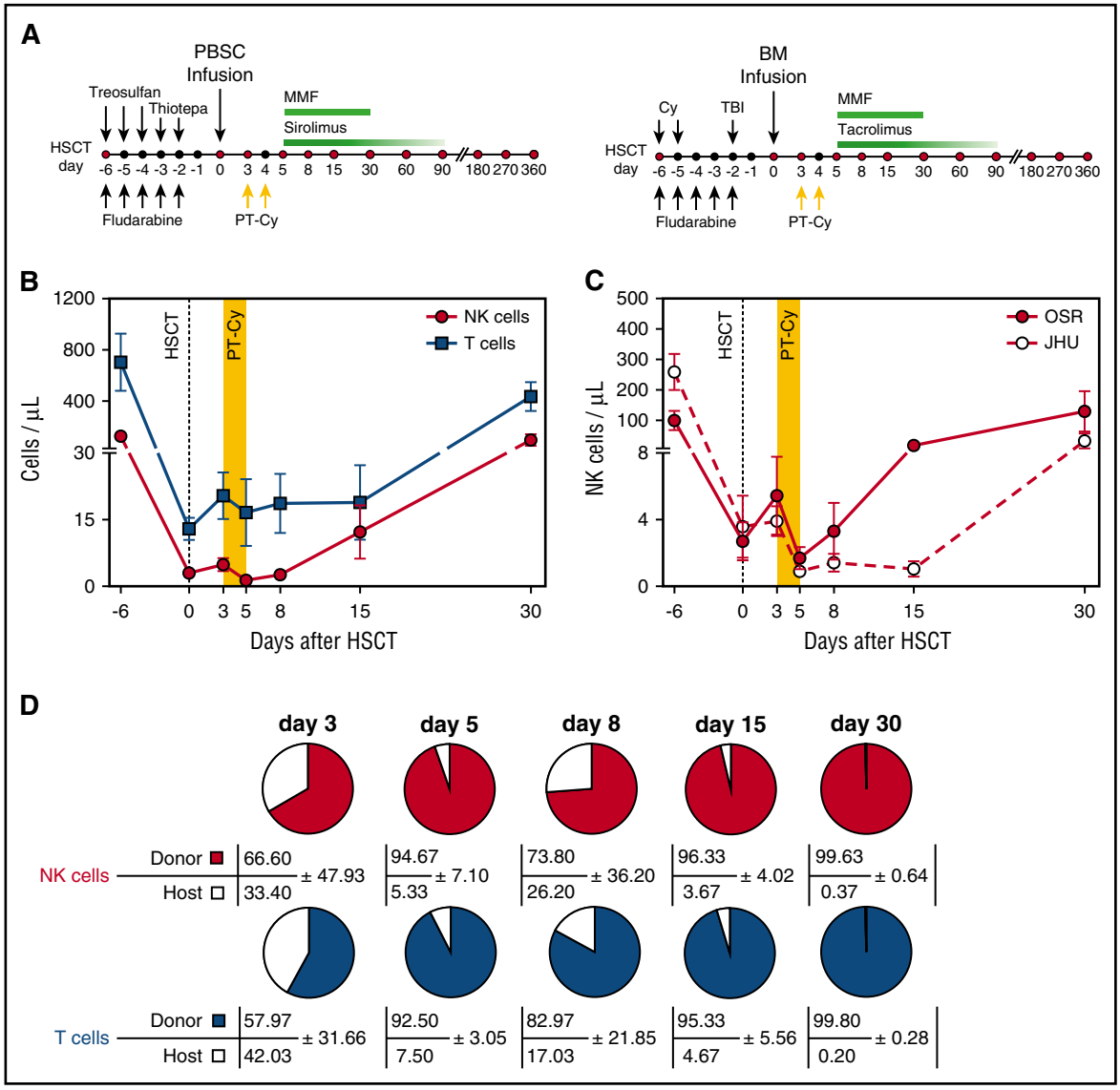

Figure 1. NK cell counts and chimerism early after haploidentical HSCT and PT-Cy. (A) Outline of the haploidentical HSCT platforms used at OSR (left) and at JHU (right). (B) Absolute counts of NK cells (red circles) and T cells (blue squares) circulating in the PB of patients (n = 17) receiving haploidentical HSCT followed by PT-Cy (days of Cy administration are shaded in yellow). Data are displayed as mean values ± standard error of the mean (SEM). (C) Absolute counts of PB NK cells in patients treated in the 2 transplantation centers (OSR, red circles: n = 10; JHU, white circles: n = 7). Data are displayed as mean values with SEM. (D) Chimerism within T- and NK-cell compartment after HSCT. HLA-A*02 mismatches allowed to discriminate by multiparametric flow cytometry donor-derived cells (colored) and residual host lymphocytes (white). Pies depict NK cell (upper line) and T cell (bottom lines) chimerism measured at different time points after HSCT in 3 donor-recipient pairs. Numbers indicate mean values with standard deviation (SD). MMF, mycophenolate mofetil; PBSC, peripheral blood cell transplantation; TBI, total body irradiation.

haploidentical HSCT with a GVHD prophylaxis based on PT-Cy, and to investigate whether NK cell alloreactivity is preserved in this innovative and increasingly used transplant modality.

Materials and methods

Multiparametric flow cytometry

Absolute quantification of NK ($CD3^-CD56^+$) and T ($CD3^+$) cells was performed in fresh whole blood samples as previously described.[11]

For extended phenotypic analyses, mononuclear cells were isolated from peripheral blood (PB) or bone marrow (BM) by density gradient separation (Lymphoprep; Fresenius). Details on antibodies and panel assembly are provided in the supplemental Methods on the *Blood* Web site. Acquisition was performed on an LSR Fortessa and an LSRII instrument (both from BD Biosciences). Analysis was performed using FlowJo (TreeStar) and visualized as heatmaps using the pheatmap function in R. Data were further analyzed using the Barnes-Hut stochastic neighbor embedding (bh-SNE) algorithm (using the CYT tool and the MatLab software as described previously[12]). The input dataset was resampled to obtain an equal number of NK cell events for all of the samples analyzed; the bidimensional maps obtained from this analysis were then processed with FlowJo software to highlight the spatial distribution of NK cells at each time point. Upon bh-SNE analysis,[12] the k-means algorithm was used for unsupervised clustering of data to identify and quantify in an unbiased manner memory-like NK cells in patient and healthy donor samples.

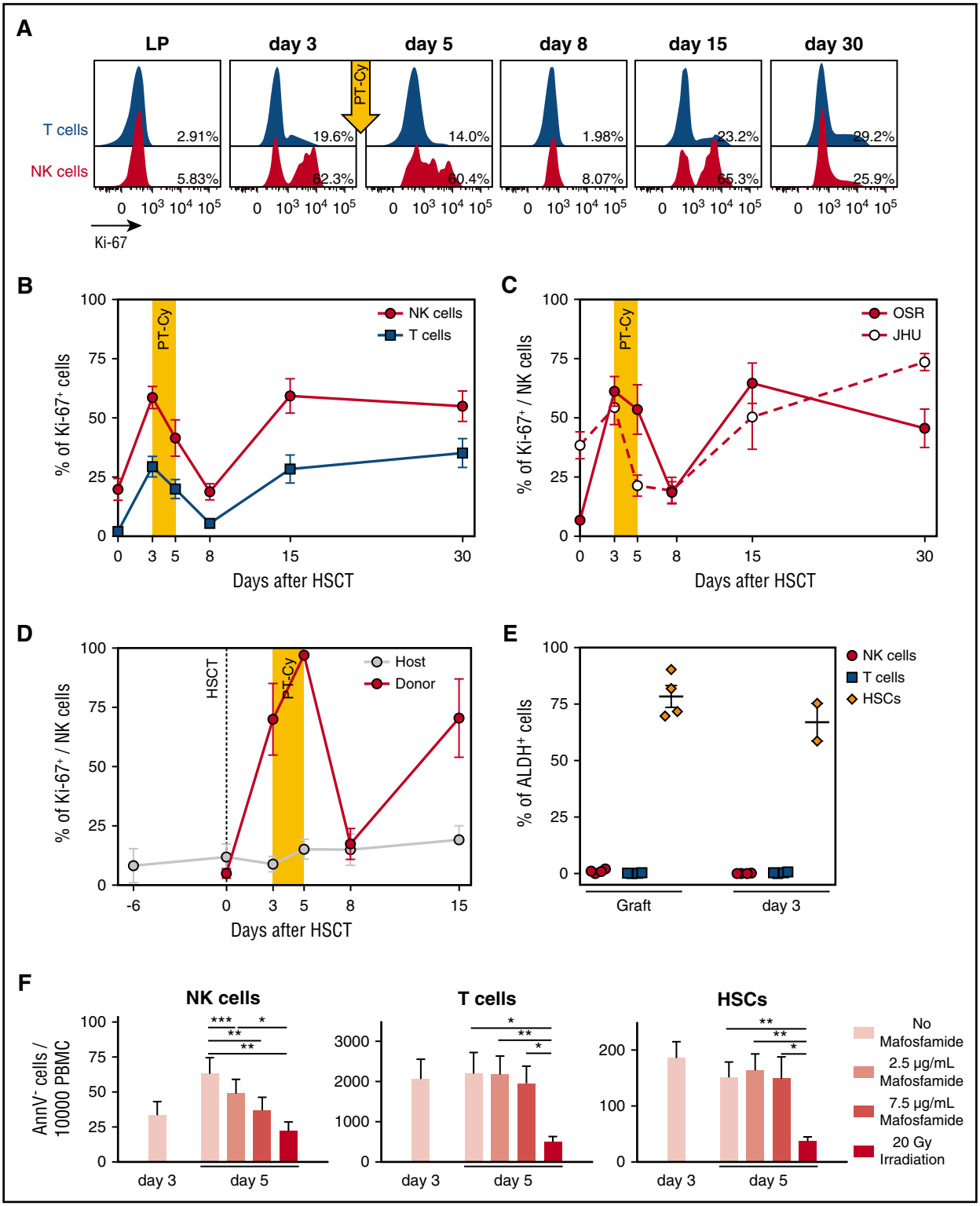

Figure 2. Cyclophosphamide administration induces killing of proliferating NK cells. (A) Flow cytometry histograms depicting Ki-67 expression measured on T (blue) and NK cells (red) from the leukapheresis (LP) graft and in the PB of a representative patient (OSR #1) at different time points after HSCT, as indicated. Percentages indicate frequencies of Ki-67–positive cells. (B) Ki-67 positivity in NK (red circles) and T (blue squares) cells from the graft (day 0), or circulating in the PB of patients after HSCT with PT-Cy (n = 17). (C) Ki-67 positivity in NK cells from the graft (day 0) or in the PB of patient transplanted at OSR (red circles: n = 10) or JHU (white circles: n = 7). (D) Level of proliferation of donor-derived NK cells (red circles) and residual host NK cells (gray circles) measured with Ki-67 intracellular staining in 3 representative patients. Donor- or host-derived NK cells were discriminated by immunophenotypic analysis using differential expression of the mismatched HLA-A*02 allele. (E) Scatter plot depicting the mean percentage of ALDH$^+$ cells detected by flow cytometry among NK (red circles), T (blue squares), and stem (orange diamonds) cells present within the infused graft, or in the patient PB 3 days after transplant, in 4 representative patients. Note that for 2 of 4 patients, CD34$^+$ stem cells were no more detectable in the patient PB at day 3. (F) In vitro assay of mafosfamide-induced cell death. The LP product of 6 patients was stimulated with IL-15 at day 0 and treated with different doses of mafosfamide at day 3. The graphs report the number of viable (AnnexinV$^-$) NK cells, T cells, and HSCs detected by flow cytometry before the treatment (day 3) and after administration of different doses of the drug (day 5; light pink bars: untreated; dark pink bars: 2.5 µg/mL; light red bars: 7.5 µg/mL) and after irradiation as positive control (day 5, red bars). Unless otherwise specified, shown in all panels are average values ± SEM.

Mafosfamide-sensitivity assay

An in vitro assay to test the effect of mafosfamide on NK cells was adapted from a published protocol.[13] Briefly, cryopreserved PB mononuclear cells obtained from a donor's graft were thawed, marked with Cell Trace Violet (CTV, Life Technologies), and cultured in Iscove modified Dulbecco medium (Lonza) supplemented with 10% human serum (Euroclone), 1% penicillin streptomycin, 1% glutamine (Lonza), and 5 μg/mL interleukin-15 (IL-15, Miltenyi). Mafosfamide L-lysine salt (Niomech) was diluted in distilled water and added to the culture after 3 days. After 1 hour of incubation, cells were centrifuged twice and then plated in fresh medium supplemented with IL-15. CTV dilution and quantification of live nonapoptotic cells (Annexin V^-) were assessed by flow cytometry, before (day 3) and 2 days after (day 5) adding mafosfamide. The same experiment was performed in the absence of CTV labeling to analyze proliferation using Ki-67 intracellular staining.

Cytotoxicity assay

Cryopreserved PB mononuclear cells obtained from HSC donors before granulocyte colony-stimulating factor mobilization, from patients at day 30 after HSCT, and from healthy subjects, were thawed and plated in Iscove modified Dulbecco medium supplemented with 10% human serum in the presence of 20 IU/mL of recombinant human IL-2 (Novartis). After overnight incubation, NK cells were isolated by negative selection with anti-CD3, anti-CD14, and anti-CD19 magnetic beads (Miltenyi), labeled with CTV and plated in a 50:1, 10:1, or 1:1 effector:target ratio in the presence of the following targets: K562 cell line, OCI/AML3 cell line, and primary AML blasts collected from a patient at diagnosis (90% purity). After a 6-hour incubation, apoptosis of CTV-negative target cells was analyzed by assessing Annexin V (Biolegend) expression by flow cytometry.

Statistical analyses

A detailed description of statistical analyses performed to compare experimental data and patient outcome is provided in the supplemental Methods.

Results

NK cell recovery displays similar metrics in different PT-Cy–based haploidentical HSCT protocols

To assess NK cell dynamics after haploidentical T cell–replete HSCT with PT-Cy, we analyzed PB and BM samples collected longitudinally in time from 17 patients treated over the same period in 2 transplantation centers (Ospedale San Raffaele, Milano, Italy [OSR]; John Hopkins University, Baltimore, MD [JHU]). Patient and transplant characteristics are provided in the supplemental Methods and summarized in Table 1; HSCT platforms are outlined in Figure 1A.

After infusion of the graft, which for all patients included an elevated content of mature donor NK cells (median, 9.18× 10^6/kg; range, 1.66-26.2 × 10^6/kg), absolute T-cell and NK cell counts were measured in PB before (day 3) and after (days 5, 8, 15, and 30) cyclophosphamide administration (Figure 1A-B). As previously reported,[14-16] T and NK cells were detectable at very low levels even immediately after graft infusion. PT-Cy treatment resulted in a further decrease of cell counts, with residual NK cells barely detectable at day 5. After that, T and NK cells progressively increased at days 15 and 30 after HSCT. Patients treated in the 2 transplant centers displayed similar in vivo dynamics, with a slight delay in recovery in JHU patients (Figure 1C). To assess the origin of the circulating NK cells, we analyzed lymphocyte chimerism in 3 donor-recipient pairs mismatched for

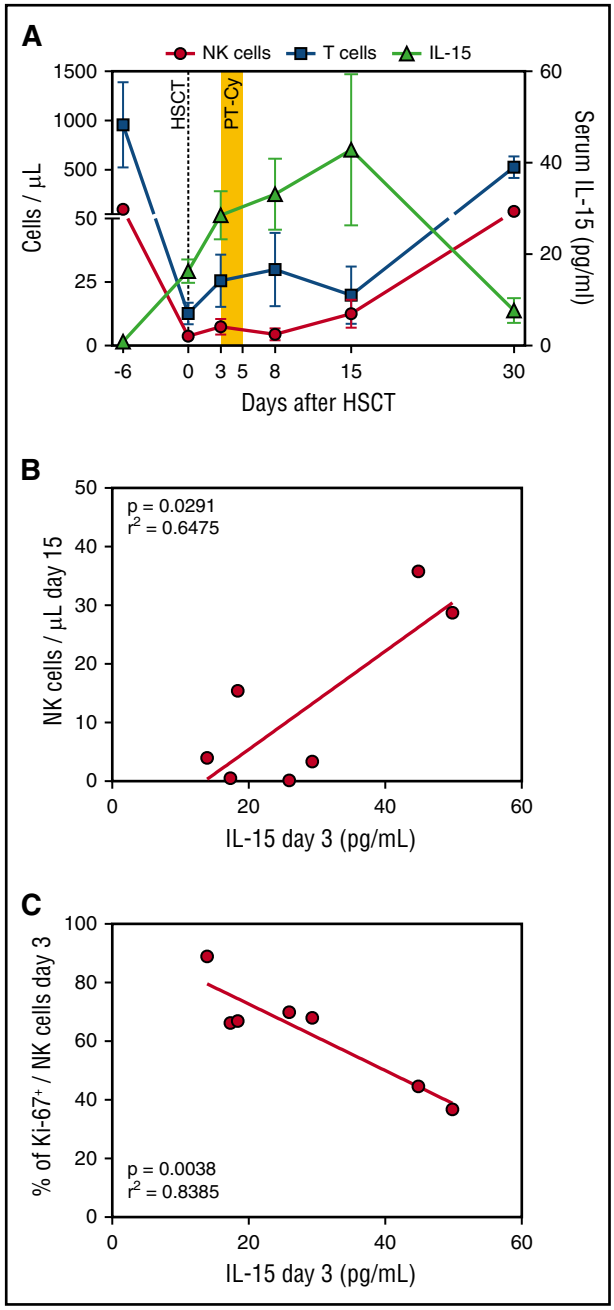

Figure 3. IL-15 serum levels sharply increase after HSCT and cyclophosphamide administration and correlate with NK cell dynamics. (A) IL-15 concentration (green triangles) measured in the sera of 7 patients before and after HSCT with PT-Cy is shown with the number of NK cells (red circles) and T cells (blue squares) in the PB of the same patients. Mean values with SEM are shown. (B) Correlation between IL-15 serum concentration at 3 days after HSCT (x-axis) and NK cell counts at day 15 after HSCT (y-axis). The red line denotes the best-fit line of the linear regression analysis. (C) Correlation between IL-15 serum concentration at 3 days after HSCT (x-axis) and the percentage of NK cells proliferating at the same time point, measured by Ki-67 intracellular staining (y-axis). The red line denotes the best-fit line of the linear regression analysis.

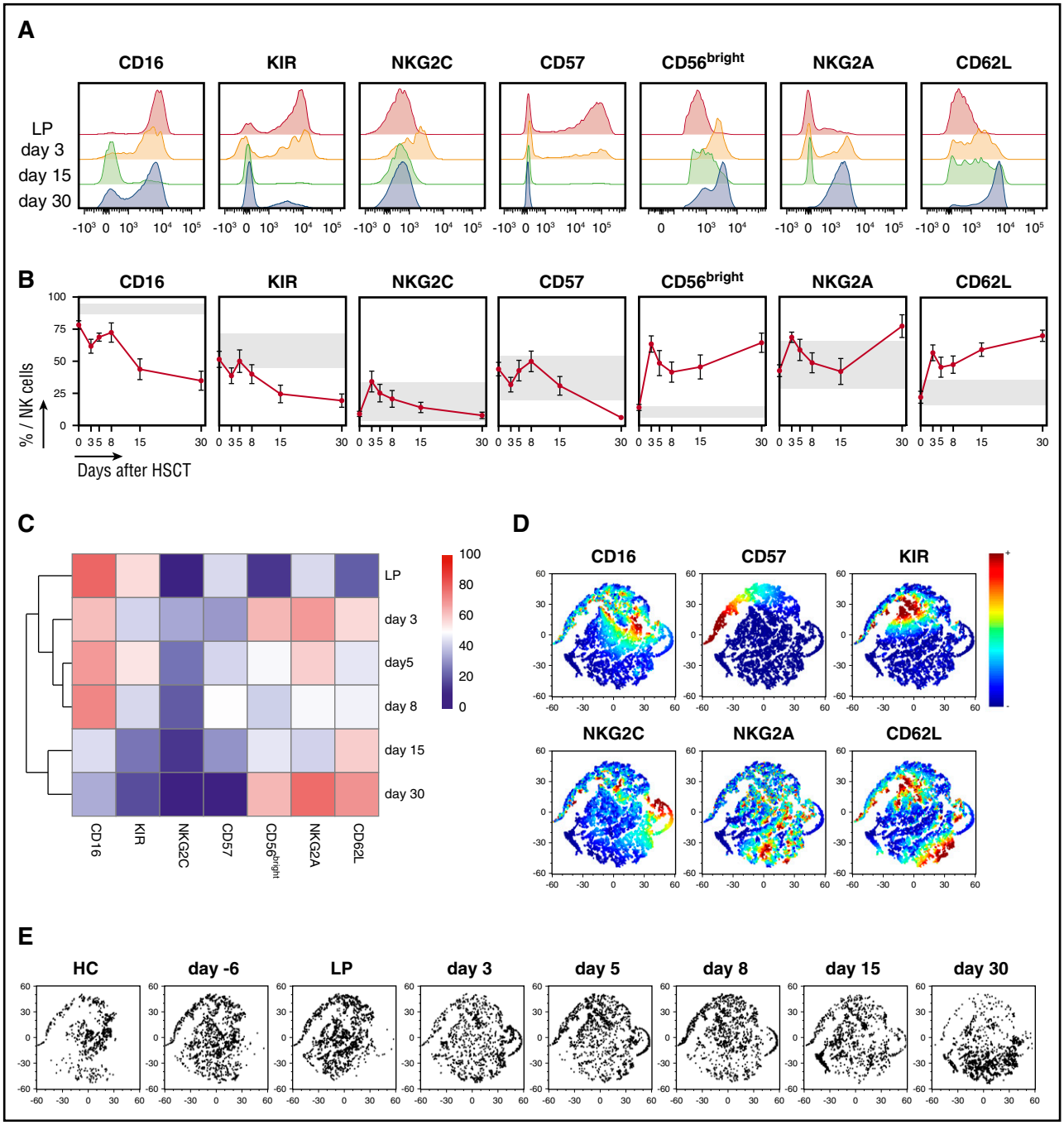

Figure 4. The second wave of NK cells that appear after PT-Cy displays an immature phenotype. (A) Flow cytometry histograms depicting expression of indicated maturation markers on CD56$^+$ CD3$^-$ NK cells from a representative patient (OSR #1) at the indicated time points (LP: red; day 3: orange; day 15: green; day 30: blue). (B) The expression of the described maturation markers measured by flow cytometry in NK cells from the graft (day 0) and from patients longitudinally sampled after HSCT with PT-Cy (n = 10). For each marker, a normal reference interval (mean ± SD) measured in NK cells from 5 healthy subjects is displayed (gray box). (C) Heat map of the average NK cell maturation marker expression at different time points, with unsupervised hierarchical clustering, for 10 OSR patients analyzed by multiparametric flow cytometry at the indicated time points. (D-E) Multidimensional single-cell analysis of the maturation status of NK cells harvested from 5 healthy controls (HC), from leukapheresis (LP, n = 10) and from 10 patients at different time points after HSCT. The panel D bidimensional maps were obtained from flow cytometric data using the bh-SNE algorithm show all analyzed NK cell events, with coloring denoting the expression of each maturation marker, as indicated. The same data are depicted in panel E, where NK cells from a selected time point are displayed separately.

HLA-A*02. In both the T- and NK-cell compartments, donor-derived lymphocytes accounted for the majority of cells even at early time points (Figure 1D); host-derived lymphocytes became undetectable by day 30. A minor deflection of chimerism was observed at day 8, suggesting a preferential sensitivity of donor-derived cells to PT-Cy administration.

PT-Cy eliminates proliferating donor-derived NK cells in vitro and in vivo

Cyclophosphamide is an alkylating agent known to be particularly active on dividing immune cells.[7,17] We thus used Ki-67 staining to investigate the effects of PT-Cy on NK cell proliferation. At day 3 after transplantation, NK cells robustly proliferated, even

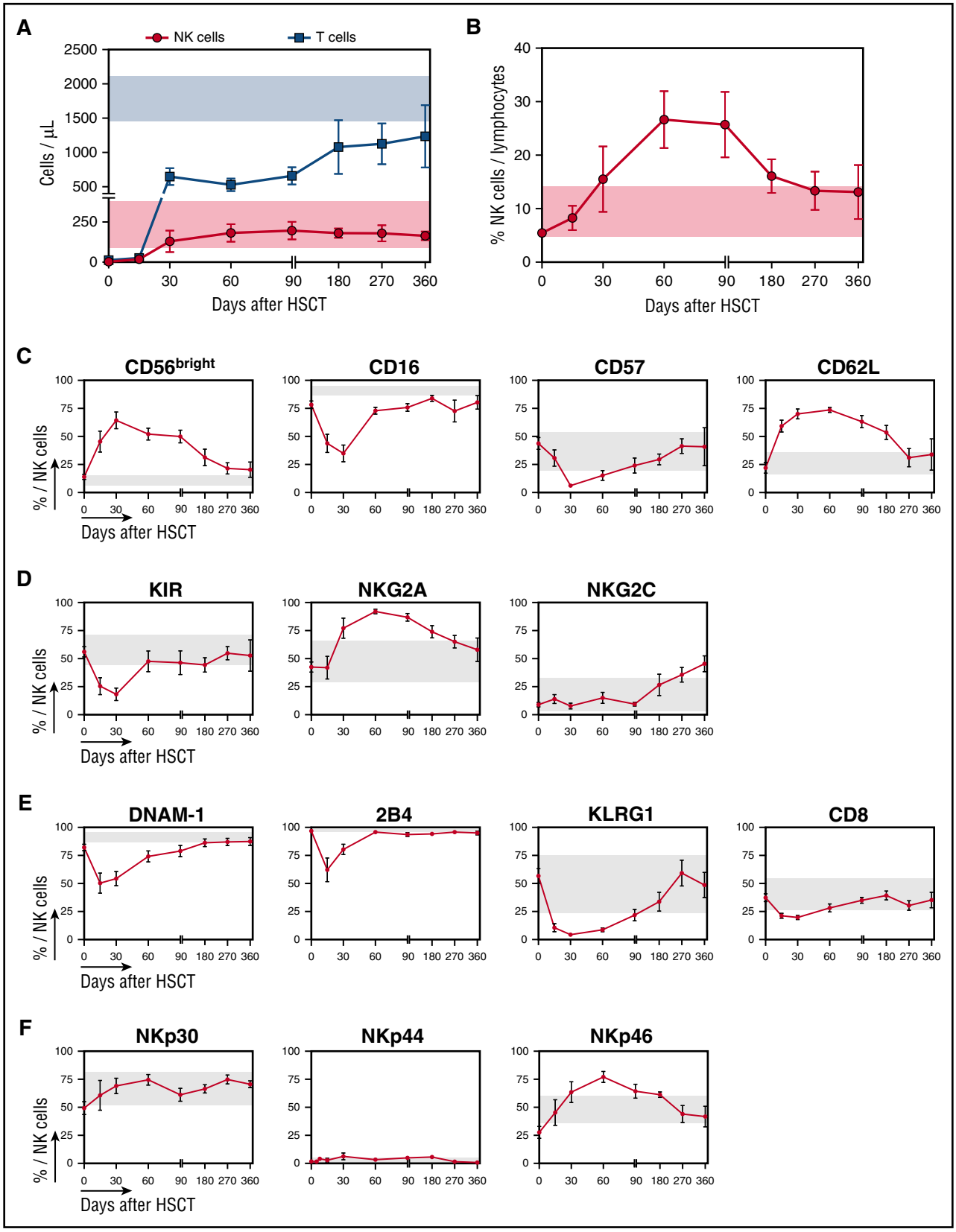

Figure 5. Despite early recovery of NK cell counts after PT-Cy–based HSCT, NK cell phenotype normalization occurs only several months after transplantation. (A) Absolute counts of NK cells (red circles) and T cells (blue squares) detected in the PB of 10 patients followed long-term after HSCT with PT-Cy (from days 30 to 360). A reference physiological cell count interval (mean ± SD) obtained from 5 healthy controls is shown for NK cells (light red box) and T cells (light blue box). (B) The proportion of NK cells out of total lymphocytes in the infused donor graft (day 0) and longitudinally after HSCT is displayed for 10 OSR patients. (C-F) Flow cytometry histograms depicting the expression of selected markers on $CD56^{+}CD3^{-}$ NK cells in the donor graft (day 0) or from patient PB obtained longitudinally after transplant in

to a higher extent than T cells (Figure 2A-B). As previously described for T lymphocytes,[14,15] we found that NK cell proliferation was completely abrogated by day 8, suggesting selective elimination of cycling NK cells. Importantly, similar NK cell proliferation kinetics were observed in patients from the 2 centers (Figure 2C), suggesting that this dynamic is minimally influenced by differences in graft source, conditioning intensity, and subsequent pharmacological GVHD prophylaxis. Interestingly, in patients in which the donor or host origin of circulating NK cells could be assessed through the expression of mismatched HLA-A*02, we found that the in vivo proliferation was largely restricted to donor-derived NK cells (Figure 2D).

These observations suggested that actively proliferating donor-derived NK cells were selectively eliminated upon cyclophosphamide administration. In line with this hypothesis, we failed to record any activity of ALDH, an enzyme known to confer intrinsic resistance to Cy,[13,18,19] in NK cells contained within the graft or in PB samples collected at day 3 after infusion (Figure 2E).

To directly demonstrate that proliferating NK cells are selectively eliminated by Cy, we mimicked in vitro the transplantation protocol by prompting the proliferation of NK cells with recombinant human IL-15 and challenging them after 3 days with mafosfamide, a Cy analog suitable for in vitro use. After 2 additional days, proliferating NK cells had been eliminated by mafosfamide in a dose-dependent manner, as demonstrated by a progressive decrease in the counts of viable cells (Figure 2F) and in the abrogation of proliferation (supplemental Figure 1A-C). Conversely, T cells and $CD34^+$ stem cells from the graft did not proliferate in these experimental conditions and were consequently not eliminated by in vitro administration of the drug. Overall, these data demonstrate that NK cells contained in the graft proliferate robustly upon infusion into patients, and that the proliferation state and lack of ALDH of these NK cells jointly cause them to be purged in vivo by PT-Cy.

IL-15 serum levels peak after PT-Cy administration and correlate with the kinetics of NK cell recovery

IL-15 is a "4 α-helix bundle" cytokine primarily produced by monocytes, macrophages, and dendritic cells, and is known to play a pivotal role in lymphocyte homeostasis and especially in NK cell development, maturation, and proliferation.[20] In a lymphodepleted environment, such as the one established in patients after conditioning, elevated IL-15 levels can affect the fate and the function of the infused donor NK cells.[21,22] We thus measured the serum concentration of IL-15 longitudinally during the first months after haploidentical HSCT with PT-Cy (details provided in supplemental Methods).

Systemic levels of IL-15 rose immediately after conditioning (Figure 3A), possibly favoring the donor NK cell proliferation seen early after graft infusion (Figure 2B). Interestingly, the high levels of IL-15 documented at day 3 displayed a direct correlation with the number of NK cells reconstituting thereafter (Figure 3B) and an inverse correlation with the frequency of NK cells proliferating at the same time point (Figure 3C). A potential explanation is that higher early proliferation of NK cells consumes IL-15, leading to lower measurable levels in these patients. Starting from day 15, a second wave of highly proliferating donor NK cells appeared in the PB of patients, followed by a drop in IL-15 levels at day 30, suggesting again consumption of the cytokine by reconstituting lymphocytes.

Although much remains to be discovered about the factors that regulate NK cell dynamics in the early posttransplantation phase, these findings highlight that the cytokine milieu early after haploidentical HSCT with PT-Cy include high levels of IL-15, and that these are significantly correlated with the metrics of NK cell recovery.

Second wave of reconstituting NK cells appears 2 weeks after HSCT with PT-Cy and predominantly consists of cells with an immature phenotype

Our analysis of absolute counts (Figure 1B-C) and proliferation kinetics (Figure 2B-C) of NK cells after haploidentical HSCT and PT-Cy demonstrated that a sizeable population of highly proliferating NK cells becomes evident around day 15 after HSCT. To evaluate the ability of these cells to provide an effective protection against pathogens and disease recurrence, we assessed their phenotypical features and maturation status. The expression of maturation markers was assessed through multiparametric flow cytometry on NK cells contained within the donor leukapheresis (shown as day 0 in Figure 4B), and on patient PB NK cells immediately after HSCT (day 3) and after PT-Cy (days 5, 8, 15, and 30). The results for OSR patients are shown in Figure 4A-B; JHU patient results appear in supplemental Figure 2A-B.

As expected, NK cells in the donor graft exhibited high expression of markers associated with a mature phenotype (CD16, KIR, NKG2C, and CD57) and low expression of markers of immature NK cells (NKG2A and CD62L). Although the phenotype of NK cells circulating in the PB of patients immediately after HSCT (day 3, Figure 4A-B) resembled that of infused NK cells, the NK cell phenotype seen after PT-Cy administration was significantly different. By day 8, in fact, expression of maturation markers on NK cells became low or absent, whereas the percentage of $CD56^{bright}$ NK cells and the overall expression of NKG2A and CD62L increased. Unsupervised clustering of fluorescence-activated cell sorter data demonstrated clear differences between NK cells found in the graft and in patients immediately after transplant compared with patient NK cells at days 15 and 30, both in OSR and in JHU patients (Figure 4C; supplemental Figure 2A-C).

To validate these findings, the same flow cytometry data were analyzed using the bh-SNE algorithm for unbiased high-dimensional analysis.[12] NK cell events from all samples were plotted together on a bidimensional map based on the similarities of expression of maturation markers (Figure 4D). NK cells harvested from healthy subjects, grafts, patients pretransplant, and at the early time points after HSCT (from days 3 to 8) clustered in the upper portion of the multidimensional map (Figure 4E), characterized

Figure 5 (continued) 10 OSR patients. For all panels, gray boxes show reference values (mean ± SD) obtained analyzing 5 healthy controls. (C) Expression of maturation markers. (D) Expression of KIRs and lectin-type receptors. (E) Expression of markers of exhaustion or activation. (F) Expression of natural cytotoxicity receptors. Unless otherwise specified, data are shown as mean ± SEM.

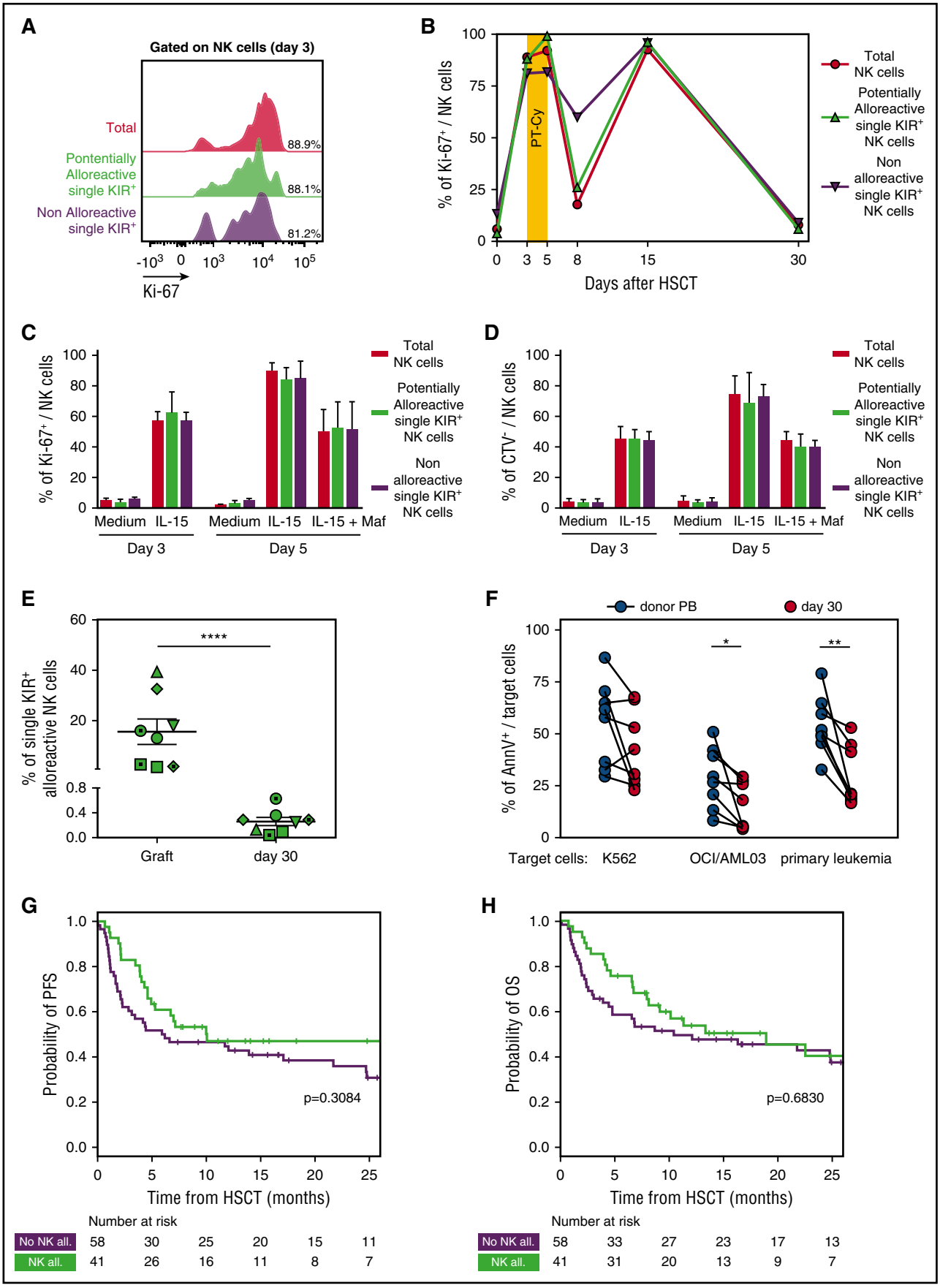

Figure 6.

by high positivity for CD16, CD57, and KIR molecules and by intermediate expression of NKG2C. Conversely, NK cells harvested from patients at days 15 and 30 after HSCT grouped in the opposite part of the map, denoting high expression of NKG2A and CD62L molecules (Figure 4D-E). Overall, these data suggest that after the rapid purging of mature proliferating lymphocytes operated by PT-Cy, the subsequent NK cell recovery occurs principally through maturation from graft progenitors rather than by homeostatic expansion of mature graft NK cells.

After haploidentical HSCT with PT-Cy, the reconstitution of a mature NK cell compartment can take up to 1 year

To address whether, and if so at what time, a mature and functional NK cell repertoire is restored, we longitudinally traced the phenotype of circulating NK cells during the first year after transplant in OSR patients. Consistent with previous reports,[23] we documented stable physiological absolute counts of circulating NK cells from 1 month after HSCT onwards (Figure 5A). Because of the relatively low number of circulating T cells in PB during the first 3 months after transplant, NK cells were the most abundant lymphocyte subset during this time (Figure 5B). Many features linked to immaturity, such as increased proportions of the CD56^{bright} subset and of CD62L^{+} NK cells, decreased over time and regained normal levels after 9 to 12 months posttransplant (Figure 5C). An opposite trend, but with different kinetics, was observed for the expression levels of the maturation markers CD16 and CD57. The expression of KIRs returned to normal levels by day 60 (Figure 5D), but, as previously reported in other HSCT settings,[24,25] the levels of the inhibitory receptor NKG2A diminished only 6 months after HSCT, suggesting that the ability of circulating NK cells to use target recognition through HLA class I-KIR interactions is not fully recovered before this time point. Of notice, we documented higher than normal expression of the activating receptors NKG2C in reconstituting NK cells from our patients, and acquisition of this receptor was even faster in patients who developed cytomegalovirus (CMV) reactivations during their posttransplant follow-up, in line with previous reports[26,27] (data not shown).

As observed for maturation markers, the expression of DNAM-1, 2B4, KLRG-1, and CD8 also rapidly decreased early after transplant and normalized 2 to 6 months after HSCT (Figure 5E). Finally, in line with other HSCT settings,[24] we did not detect any significant deviations from normal reference values in natural cytotoxicity receptor (NKp30, NKp44, and NKp46) expression in PT-Cy–based haploidentical transplant recipients (Figure 5F). Of note, throughout the entire follow-up period, the receptor repertoire appeared nearly identical between NK cells circulating in the PB and those harvested at the same time point from the BM (supplemental Figure 3). Overall, these data indicate that the phenotypic recovery of the NK cell repertoire is a long process, taking up to 1 year after haploidentical HSCT with PT-Cy, similarly to what has been reported in other HSCT settings.[24,25]

PT-Cy dampens NK cell–mediated alloreactivity, and the graft-versus-leukemia effect correlates with residual mature NK cells

In the context of T cell–depleted haploidentical HSCT, numerous studies demonstrated that donor-recipient KIR ligand mismatches can unleash reconstituting donor NK cells against residual tumor cells.[2-5] NK cell–mediated alloreactivity is, according to this model, mediated by "single-KIR^{+}" donor NK cells, expressing on their surface a sole inhibitory receptor that can bind ligands present in the donor and absent in the recipient.[24,28,29] We thus chose to explore this specific NK cell subset to address the effect of PT-Cy on NK cell–mediated alloreactivity.

Using multiparametric flow cytometry, we compared the dynamics of potentially alloreactive single-KIR^{+} NK cells with their nonalloreactive counterparts and with total NK cells. We found similarly high levels of proliferation in all 3 groups of NK cells at day 3 after graft infusion (Figure 6A) and an analogous behavior in response to PT-Cy (Figure 6B). These ex vivo observations, limited by the low number of NK cells circulating early after HSCT, were supported by in vitro experiments, in which alloreactive and nonalloreactive NK cells from PBSC grafts proliferated in a comparable manner upon exposure to IL-15, and were equally susceptible to mafosfamide (Figure 6C-D).

Indeed, we documented that single-KIR^{+} NK cells present in the graft became almost completely undetectable in the PB of patients at day 30 (0.26 $\pm$ 0.19% of total NK cells, $P < .0001$, Figure 6E).

To investigate the functional consequences of this marked reduction of single KIR^{+} after PT-Cy, we compared the antileukemic potential of NK cells purified from 8 patients at day 30 after transplant. Compared with their counterparts from the corresponding donor PB, patient NK cells displayed impaired killing of the OCI/AML03 cell line and of primary AML blasts ($P = .026$ and $P = .004$, respectively), whereas the ability to kill the HLA class I–negative K562 cell line was less affected (Figure 6F; supplemental Figure 4).

Figure 6. PT-Cy eliminates single-KIR^{+} NK cells and thus dampens NK cell–mediated alloreactivity. (A) Flow cytometry histogram depicting proliferation measured by Ki-67 expression in total NK cells (red), in single KIR^{+} NK cells predicted to be alloreactive (green), and in single-KIR^{+} NK cells predicted to be nonalloreactive (purple) in a representative patient (OSR #10) immediately before PT-Cy administration (day 3 after HSCT). (B) Time course of Ki-67 positivity in total NK cells (red circles), single-KIR^{+} NK cells predicted to be alloreactive (green triangles), or single-KIR^{+} NK cells predicted not to be alloreactive (purple triangles) from the graft (day 0) or circulating in the PB from a representative patient (OSR #10) after HSCT. (C) Percentage of Ki-67 positivity in total NK cells from 3 PBSC grafts (red), in the subset of single-KIR^{+} NK cells predicted to be alloreactive (green), or in the subset of single-KIR^{+} NK cells predicted not to be alloreactive (purple) upon 3 days of exposure to IL-15, and after subsequent addition of mafosfamide to the culture medium. (D) Percentage of proliferating cells, measured through CTV dilution, among total NK cells from 3 PBSC grafts (red), among the subset of single-KIR^{+} NK cells predicted to be alloreactive (green), and among the subset of single-KIR^{+} NK cells predicted not to be alloreactive (purple) upon 3 days of exposure to IL-15 and after subsequent addition of mafosfamide to the culture medium. (E) Frequency of predictably alloreactive single-KIR^{+} NK cells within the graft and in PB NK cells in patients 30 days after HSCT, measured in 8 donor-recipient pairs with KIR-ligand mismatches. (F) Target cell death, expressed as Annexin V positivity (AnnV^{+}), measured on K562 cells, OCI/AML cells, or primary leukemic cells after incubation at a 10:1 effector:target ratio with NK cells purified from patient PB day 30 after HSCT with PT-Cy (n = 8, red dots) or from their respective donors PB (n = 8, black dots). (G-H) Progression-free survival (G) and overall survival (H) in patients who received PT-Cy–based haploidentical HSCT from donor with (green line, n = 41) or without (purple line, n = 58) predicted NK cell alloreactivity. Tick marks represent censoring for live patients. Unless otherwise specified, data are shown in all panels as mean values $\pm$ SEM.

Table 2. Characteristics of patients analyzed for the impact of NK alloreactivity on HSCT outcome

Characteristics	Patients with predicted NK alloreactivity (n = 41)	Patients without predicted NK alloreactivity (n = 58)	*P*
Median follow-up, mo (range)	15.5 (5.2-38.6)	27.4 (3.5-44.3)	.13
Median age, y (range)	53 (21-77)	49.5 (21-76)	.54
Patient sex, n			.39
M	29	36	
F	12	22	
Disease, n			.66
AML	27	32	
ALL	2	6	
MPN	1	2	
MDS	1	5	
NHL	2	5	
HL	7	7	
MM	1	0	
Median Sorror HCT-CI (range)*	2 (0-6)	3 (0-8)	.14
Refined DRI, n†			.28
Low	3	4	
Intermediate	9	9	
High	13	19	
Very high	4	15	
Previous allogeneic HSCT	12	11	
Conditioning regimen, n‡			.36
Treo-Flu-Mel	25	34	
Thio-Treo-Flu	13	12	
Thio-Bu-Flu	0	3	
Treo-Flu	1	5	
Other	2	4	
Source of stem cells, n			.26
PB	41	55	
BM	0	3	
Graft composition			
$CD34^+$ cells × 10^6/kg, median (range)	5.6 (4-10.3)	5.4 (1.6-6.7)	.69
$CD3^+$ cells × 10^7/kg, median (range)	156 (5-400)	196 (4-729)	.02
GVHD prophylaxis, n			NA
PT-Cy, sirolimus, MMF	41 (100%)	58 (100%)	

HCT-CI, hematopoietic cell transplantation-comorbidity index; MM, multiple myeloma; MPN, myeloproliferative neoplasm; NA, not available.

*HCT-CI calculated according to Sorror et al.[50]

†DRI calculated according to Armand et al.[49]

‡Conditioning regimens: Thio-Bu-Flu, thiotepa (5 mg/kg/d on days −7 and −6), busulfan (3.2 mg/kg/d on days −5 to −3), and fludarabine (50 mg/m²/d on days −5 to −3); Treo-Flu, treosulfan (14 g/m²/d on days −6 to −4) and fludarabine (30 mg/m²/d on days −6 to −2); Treo-Flu-Mel, treosulfan (14 g/m²/d on days −6 to −4), fludarabine (30 mg/m²/d on days −6 to −2), and melphalan (70 mg/m²/d on days −2 and −1).

Although these in vitro data suggest that NK cells reconstituting early after haploidentical HSCT with PT-Cy display an impaired antileukemic potential compared with their mature donor counterparts, this small but significant difference might still be overruled by other factors in vivo. To provide more insights into this relevant issue, we analyzed the clinical impact of predicted NK alloreactivity in a cohort of 99 consecutive patients who received haploidentical HSCT at OSR. All patients received a myeloablative chemotherapy-based conditioning and a GVHD prophylaxis based on PT-Cy. KIR ligand mismatches were present in 41 of 99 patients (Table 2). In line with our expectations, and contrary to what has been consistently documented in T cell–depleted haploidentical transplants,[2-4] predicted NK cell alloreactivity did not significantly affect any of the major HSCT end points (including GVHD, relapse incidence, and survival) either in the entire cohort (Figure 6G-H; supplemental Figure 5) or in subgroup analysis (supplemental Table 2). These data suggest that by eliminating the majority of mature alloreactive NK cells transferred as part of the graft, PT-Cy dampens the impact of KIR ligand mismatches on HSCT outcome.

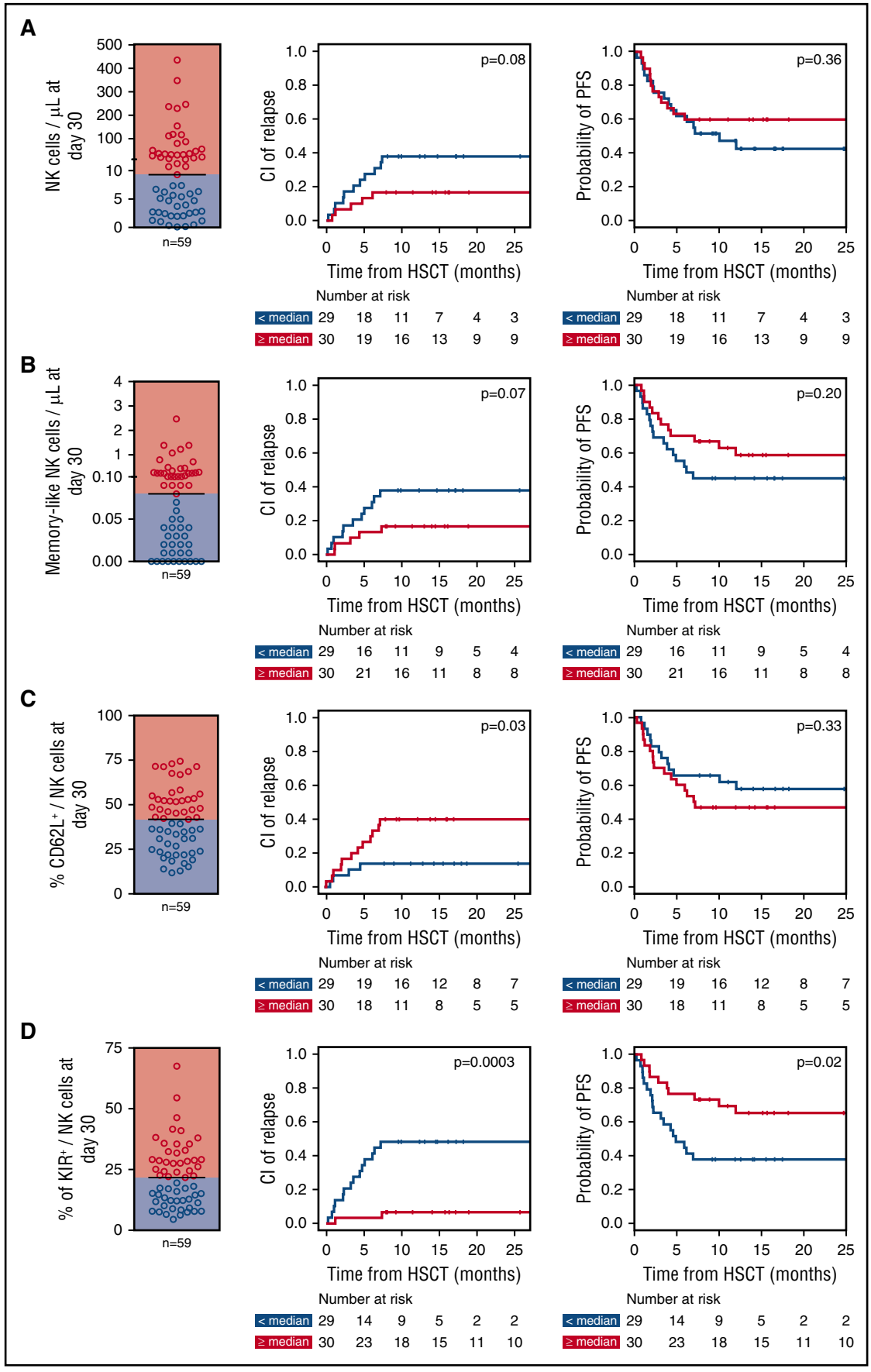

Figure 7.

Finally, to verify whether the proportion of mature NK cells spared by PT-Cy might have a clinically relevant role in determining HSCT outcome, we analyzed the maturation phenotype of NK cells circulating at day 30 after HSCT in 59 OSR patients who underwent haploidentical HSCT with PT-Cy and linked it to disease-related clinical end points. Beside the analysis of single maturation markers, we also enumerated $CD57^+CD16^+KIR^+NKG2C^+$ mature memory-like NK cells, based on unsupervised data clustering of bh-SNE data using the k-means algorithm (supplemental Figure 6). In univariate analysis, low expression of CD62L and high expression of KIRs on NK cells at day 30 after HSCT were significantly correlated with lower relapse incidence ($P = .03$ and $P = .0003$, respectively), and high absolute counts of total and memory-like NK cells displayed a trend toward significance for the same end point ($P = .08$ and $P = .07$), in line with previous reports.[30] Moreover, high expression of KIRs on NK cells at day 30 displayed a significant correlation with higher progression-free survival ($P = .02$, Figure 7A-D; supplemental Table 3). Despite the relatively small size of our patient series, the significant correlation between KIR expression on NK cells at day 30 and lower relapse incidence held true in multivariate analysis ($P = .012$; supplemental Table 4), suggesting that KIR expression might represent a clinically relevant proxy for the functional competence of reconstituting NK cells in preventing recurrence.

Discussion

By counterposing the immune systems of 2 individuals with disparate HLA and KIR assets, haploidentical HSCT represents a unique model to investigate the biological determinants of NK cell tolerance and alloreactivity and has provided convincing in vivo evidence of the immunotherapeutic potential endowed in this cell subset.[2,5,22,31] However, with the ongoing development of strategies to render HLA-mismatched transplant more feasible, it is becoming increasingly evident that the complex dynamics of NK cell recovery are dramatically affected by changes in the conditioning regimen and GVHD prophylaxis: for this reason, immunogenetic models to predict NK cell–mediated effects have to be validated in each HSCT platform.

In the present study, we integrated immunogenetic, functional, and clinical data to analyze the metrics and correlates of NK cell repertoire reconstitution in patients who received haploidentical HSCT according to 2 different PT-Cy platforms. We undertook this to address whether the models formulated in T cell–depleted haploidentical HSCT also hold true in this more recent and increasingly common transplantation modality.

We showed that the high numbers of mature NK cells infused as part of the graft in this HSCT setting immediately encounter high levels of homeostatic cytokines released as a consequence of the conditioning regimen–mediated lymphodepletion. As a result, we observed that infused NK cells are prompted to proliferate to an even higher extent than their T cell counterparts, and showed in vitro and in vivo that such proliferation confers NK cell sensitivity to Cy-mediated killing.

After the purging of the majority of mature donor NK cells from the graft by PT-Cy, we observed the appearance of a second wave of donor-derived NK cells. These cells, however, displayed phenotypic and functional features of immaturity for several months after HSCT, strongly suggesting that they might stem directly from HSCs contained in the graft rather than from the mature NK cells infused alongside them.

Although it is extremely difficult to track their complex dynamics during the early posttransplant phase because of their very low numbers, single-KIR^+ NK cells, considered to include potentially alloreactive NK cells, appeared to behave similarly to all other mature NK cells and were thus almost completely eliminated by PT-Cy. As a consequence, the most widely accepted algorithm used to predict beneficial NK alloreactivity in T cell–depleted transplants[3] failed to predict clinical outcome in our patient series. Conversely, and consistently with the role we described for PT-Cy in this setting, the absolute counts and relative proportion of mature NK cells at day 30 after HSCT appeared to be a more reliable predictor of an effective NK cell–mediated immunosurveillance against relapse in this HSCT platform.

Our results have several other practical implications: whereas, for instance, it is becoming widely accepted that transplantation from HLA-mismatched relatives represents a viable alternative for patients who lack a conventional matched donor,[9,10] the question of which donor to select among several possible family members is still debated.[32,33] Here we found that the "classical" KIR ligand mismatch model of NK cell alloreactivity did not correlate with any of the major HSCT end points in PT-Cy–based haploidentical HSCTs, indicating that, in this context, priority should be given to other donor selection criteria, including CMV serostatus, gender mismatch, and presence of donor-specific anti-HLA antibodies in the recipient. It should be considered, however, that different NK cell alloreactivity models, also taking into account the donor-recipient KIR genotype, might be needed to predict NK-mediated effects in this context, as widely accepted for HLA-matched donor HSCT,[34,35] and already proposed by other studies for the haploidentical context.[36,37]

A second observation relates to the finding of a relatively long time window in which most of the circulating NK cells display phenotypic features of immaturity. Previous reports have highlighted that, despite the relatively rapid recovery of CD8 T-cell counts, PT-Cy transplantation is often accompanied by frequent viral reactivations, including those from CMV, polyomaviruses, and human herpes virus 6.[38] We can speculate that at least part of this susceptibility might be due to the ineffective protection conferred by the immature donor-derived NK cells, and future studies should verify whether the dynamics of recovery of memory

Figure 7. Mature KIR^+ NK cells that are spared by PT-Cy can protect against posttransplantation disease relapse. (A) Absolute counts of circulating NK cells, (B) absolute counts of $CD57^+CD16^+KIR^+NKG2C^+$ memory-like NK cells, (C) percentage of $CD62L^+$ NK cells, and (D) percentage of KIR^+ NK cells were determined in samples collected at day 30 after HSCT from 59 patients who received haploidentical HSCT followed by PT-Cy at OSR. For each of these parameters, dot plots to the left of the figure display the distribution in the patient cohort, discriminating between patients with values above (red dots and background) or below (blue dots and background) the median. Curves display the cumulative incidence of disease relapse (center panels) and PFS (right panels) in each subgroup. *P* values reported in each panel corner are relative to univariate comparisons performed using Gray's test (for cumulative incidence of relapse) or log-rank test (for PFS).

NK cells could predict antiviral immune competence more effectively than currently used biomarkers.

Besides pointing out these limitations in NK cell defense intrinsic to PT-Cy–based haploidentical HSCTs, our study provides a framework to integrate new strategies to better exploit the immunotherapeutic potential of NK cells for this transplant platform.

For instance, the marked increase in IL-15 levels in the time window that immediately follows PT-Cy administration, reaching levels not commonly detected in physiological conditions, suggests that there is a temporal window here with a very favorable cytokine milieu for the in vivo expansion of alloreactive NK cells and provides the rationale for adoptive infusion of mature donor NK cells in this time frame. Of notice, several investigational trials of PT-Cy–based haploidentical HSCT followed by infusion of donor NK cells have recently been initiated and already reported promising results.[39-41]

In addition, several new agents developed to improve NK cell–mediated antileukemic responses might be integrated into PT-Cy–based haploidentical HSCTs. For instance, the recently developed anti-CD16/anti-CD33/IL-15 TriKe constructs[42] might be of benefit during the intermediate phase of recovery, when CD16 expression has been recovered but the KIR/NKG2A system has not yet reached its final equilibrium and IL-15 serum concentration has dropped to levels that might be insufficient to sustain the in vivo expansion and persistence of adoptively transferred NK cells.

An additional ground for improvement relates to the pharmacological GVHD prophylaxis used after PT-Cy administration. In accordance with the majority of current protocols for T cell–replete haploidentical HSCT, both regimens used in our study included mycophenolate mofetil during the first month after transplant: a number of studies have shown that this drug can negatively affect NK cell function[43,44]; thus, together with the in vivo purging of mature alloreactive NK cells, it might further reduce the antileukemic potential of early reconstituting NK cells. Importantly, the observed effects may also relate to other pharmacological agents and GVHD prophylaxis, an issue to be addressed in more detail in future studies.

In conclusion, our study strongly supports the notion that the complex and not yet fully elucidated dynamics of NK cell recovery after haploidentical HSCT are heavily affected by competition with other immune subsets and by the drugs used in the transplantation protocol. Whereas models of predicted NK cell alloreactivity developed in the original T cell–depleted setting held true in transplants performed with selective depletion of T-cell receptor αβ positive T cells from the graft,[45] or with coinfusion of donor-derived regulatory and conventional T cells,[46,47] the same algorithms were unable to predict outcome in the context of GIAC protocols[48] or, as shown in this report, in PT-Cy–based transplants.[36,37] In the dawning era of "personalized" haploidentical transplants, it is necessary to adapt tools to predict outcome to an informed analysis of the dynamics of immune recovery in each HSCT setting and to leverage this knowledge to develop appropriate adjunctive strategies to improve HSCT outcome.

Acknowledgments

Work at Ospedale San Raffaele was supported by grants from the Italian Ministry of Health (RF-2011-02351998, RF-2011-02348034, and TRANSCAN HLALOSS), the Associazione Italiana per la Ricerca sul Cancro (Start-Up Grant #14162), the ASCO Conquer Cancer Foundation (2014 Young Investigator Award), and the DKMS Mechtild Harf Foundation. G.O. was supported by a Fondazione Matarelli fellowship from the Associazione Italiana Leucemie and by a Fondazione Umberto Veronesi fellowship. Work at Johns Hopkins University was supported by the National Institutes of Health National Heart, Lung, and Blood Institute (grant R01HL110907) (L.L.) and by Wenner-Gren Foundation fellowship (S.B.).

Authorship

Contribution: A.R., G.O., F.C., L.L., and L.V. designed the study. A.R., G.O., S.B., V.G., N.C., C.T., and L.Z. performed experiments. R.G., S.P., M.M., F.G., A.A., M.T.L.S., J.P., L.L., and F.C. collected and analyzed patient clinical data. A.R., F.L. and S.P. performed statistical analyses, C.B. provided scientific counseling, A.R., G.O., F.C., L.L., and L.V. wrote the paper. All authors read and approved the final version of the manuscript.

Conflict-of-interest disclosure: The authors declare no competing financial interests.

The current affiliation for N.C. is the University of Milan, Milan, Italy.

Correspondence: Fabio Ciceri, Hematology and Bone Marrow Transplantation Unit, San Raffaele Scientific Institute, via Olgettina 60, Milano, Italy; e-mail: ciceri.fabio@hsr.it.

Footnotes

Submitted 8 May 2017; accepted 30 September 2017. Prepublished online as *Blood* First Edition paper, 6 October 2017; DOI 10.1182/blood-2017-05-780668.

*A.R. and G.O. contributed equally to this study.

†L.L. and L.V. contributed equally to this study.

The online version of this article contains a data supplement

There is a *Blood* Commentary on this article in this issue.

The publication costs of this article were defrayed in part by page charge payment. Therefore, and solely to indicate this fact, this article is hereby marked "advertisement" in accordance with 18 USC section 1734.

REFERENCES

1. Kanakry CG, Fuchs EJ, Luznik L. Modern approaches to HLA-haploidentical blood or marrow transplantation. *Nat Rev Clin Oncol*. 2016;13(1):10-24.

2. Mancusi A, Ruggeri L, Velardi A. Haploidentical hematopoietic transplantation for the cure of leukemia: from its biology to clinical translation. *Blood*. 2016;128(23):2616-2623.

3. Ruggeri L, Capanni M, Urbani E, et al. Effectiveness of donor natural killer cell alloreactivity in mismatched hematopoietic transplants. *Science*. 2002;295(5562):2097-2100.

4. Ruggeri L, Mancusi A, Capanni M, et al. Donor natural killer cell allorecognition of missing self in haploidentical hematopoietic transplantation for acute myeloid leukemia: challenging its predictive value. *Blood*. 2007;110(1):433-440.

5. Locatelli F, Pende D, Mingari MC, et al. Cellular and molecular basis of haploidentical hematopoietic stem cell transplantation in the successful treatment of high-risk leukemias: role of alloreactive NK cells. *Front Immunol*. 2013;4:15.

6. Luznik L, O'Donnell PV, Symons HJ, et al. HLA-haploidentical bone marrow transplantation for hematologic malignancies using nonmyeloablative conditioning and high-dose, posttransplantation cyclophosphamide. *Biol*

Blood Marrow Transplant. 2008;14(6):641-650.

7. Luznik L, O'Donnell PV, Fuchs EJ. Post-transplantation cyclophosphamide for tolerance induction in HLA-haploidentical bone marrow transplantation. *Semin Oncol*. 2012;39(6):683-693.

8. Robinson TM, O'Donnell PV, Fuchs EJ, Luznik L. Haploidentical bone marrow and stem cell transplantation: experience with post-transplantation cyclophosphamide. *Semin Hematol*. 2016;53(2):90-97.

9. Passweg JR, Baldomero H, Bader P, et al. Use of haploidentical stem cell transplantation continues to increase: the 2015 European Society for Blood and Marrow Transplant activity survey report. *Bone Marrow Transplant*. 2017;52(6):811-817.

10. Apperley J, Niederwieser D, Huang X-J, et al. Haploidentical hematopoietic stem cell transplantation: a global overview comparing Asia, the European Union, and the United States. *Biol Blood Marrow Transplant*. 2016;22(1):23-26.

11. Oliveira G, Ruggiero E, Stanghellini MTL, et al. Tracking genetically engineered lymphocytes long-term reveals the dynamics of T cell immunological memory [published correction appears in *Sci Transl Med*. 2015;7(319):319er9]. *Sci Transl Med*. 2015;7(317):317ra198.

12. Amir AD, Davis KL, Tadmor MD, et al. viSNE enables visualization of high dimensional single-cell data and reveals phenotypic heterogeneity of leukemia. *Nat Biotechnol*. 2013;31(6):545-552.

13. Kanakry CG, Ganguly S, Zahurak M, et al. Aldehyde dehydrogenase expression drives human regulatory T cell resistance to post-transplantation cyclophosphamide. *Sci Transl Med*. 2013;5(211):211ra157.

14. Cieri N, Oliveira G, Greco R, et al. Generation of human memory stem T cells after haploidentical T-replete hematopoietic stem cell transplantation. *Blood*. 2015;125(18):2865-2874.

15. Roberto A, Castagna L, Zanon V, et al. Role of naive-derived T memory stem cells in T-cell reconstitution following allogeneic transplantation. *Blood*. 2015;125(18):2855-2864.

16. Kanakry CG, Coffey DG, Towlerton AMH, et al. Origin and evolution of the T cell repertoire after posttransplantation cyclophosphamide. *JCI Insight*. 2016;1(5):e86252.

17. Winkelstein A. Mechanisms of immunosuppression: effects of cyclophosphamide on cellular immunity. *Blood*. 1973;41(2):273-284.

18. Kastan MB, Schlaffer E, Russo JE, Colvin OM, Civin CI, Hilton J. Direct demonstration of elevated aldehyde dehydrogenase in human hematopoietic progenitor cells. *Blood*. 1990;75(10):1947-1950.

19. Jones RJ, Barber JP, Vala MS, et al. Assessment of aldehyde dehydrogenase in viable cells. *Blood*. 1995;85(10):2742-2746.

20. Mishra A, Sullivan L, Caligiuri MA. Molecular pathways: interleukin-15 signaling in health and in cancer. *Clin Cancer Res*. 2014;20(8):2044-2050.

21. Dudley ME, Yang JC, Sherry R, et al. Adoptive cell therapy for patients with metastatic melanoma: evaluation of intensive myeloablative chemoradiation preparative regimens. *J Clin Oncol*. 2008;26(32):5233-5239.

22. Miller JS, Soignier Y, Panoskaltsis-Mortari A, et al. Successful adoptive transfer and in vivo expansion of human haploidentical NK cells in patients with cancer. *Blood*. 2005;105(8):3051-3057.

23. Cieri N, Greco R, Crucitti L, et al. Post-transplantation cyclophosphamide and sirolimus after haploidentical hematopoietic stem cell transplantation using a treosulfan-based myeloablative conditioning and peripheral blood stem cells. *Biol Blood Marrow Transplant*. 2015;21(8):1506-1514.

24. Vago L, Forno B, Sormani MP, et al. Temporal, quantitative, and functional characteristics of single-KIR-positive alloreactive natural killer cell recovery account for impaired graft-versus-leukemia activity after haploidentical hematopoietic stem cell transplantation. *Blood*. 2008;112(8):3488-3499.

25. Shilling HG, McQueen KL, Cheng NW, Shizuru JA, Negrin RS, Parham P. Reconstitution of NK cell receptor repertoire following HLA-matched hematopoietic cell transplantation. *Blood*. 2003;101(9):3730-3740.

26. Della Chiesa M, Muccio L, Moretta A. CMV induces rapid NK cell maturation in HSCT recipients. *Immunol Lett*. 2013;155(1-2):11-13.

27. Foley B, Cooley S, Verneris MR, et al. Cytomegalovirus reactivation after allogeneic transplantation promotes a lasting increase in educated NKG2C+ natural killer cells with potent function. *Blood*. 2012;119(11):2665-2674.

28. Anfossi N, André P, Guia S, et al. Human NK cell education by inhibitory receptors for MHC class I. *Immunity*. 2006;25(2):331-342.

29. Pende D, Marcenaro S, Falco M, et al. Anti-leukemia activity of alloreactive NK cells in KIR ligand-mismatched haploidentical HSCT for pediatric patients: evaluation of the functional role of activating KIR and redefinition of inhibitory KIR specificity. *Blood*. 2009;113(13):3119-3129.

30. Cichocki F, Cooley S, Davis Z, et al. CD56dimCD57+NKG2C+ NK cell expansion is associated with reduced leukemia relapse after reduced intensity HCT. *Leukemia*. 2016;30(2):456-463.

31. Rubnitz JE, Inaba H, Ribeiro RC, et al. NKAML: a pilot study to determine the safety and feasibility of haploidentical natural killer cell transplantation in childhood acute myeloid leukemia. *J Clin Oncol*. 2010;28(6):955-959.

32. McCurdy SR, Fuchs EJ. Selecting the best haploidentical donor. *Semin Hematol*. 2016;53(4):246-251.

33. Chang Y-J, Luznik L, Fuchs EJ, Huang X-J. How do we choose the best donor for T-cell-replete, HLA-haploidentical transplantation? *J Hematol Oncol*. 2016;9(1):35.

34. Venstrom JM, Pittari G, Gooley TA, et al. HLA-C-dependent prevention of leukemia relapse by donor activating KIR2DS1. *N Engl J Med*. 2012;367(9):805-816.

35. Cooley S, Weisdorf DJ, Guethlein LA, et al. Donor selection for natural killer cell receptor genes leads to superior survival after unrelated transplantation for acute myelogenous leukemia. *Blood*. 2010;116(14):2411-2419.

36. Symons HJ, Leffell MS, Rossiter ND, Zahurak M, Jones RJ, Fuchs EJ. Improved survival with inhibitory killer immunoglobulin receptor (KIR) gene mismatches and KIR haplotype B donors after nonmyeloablative, HLA-haploidentical bone marrow transplantation. *Biol Blood Marrow Transplant*. 2010;16(4):533-542.

37. Bastos-Oreiro M, Anguita J, Martínez-Laperche C, et al. Inhibitory killer cell immunoglobulin-like receptor (iKIR) mismatches improve survival after T-cell-repleted haploidentical transplantation. *Eur J Haematol*. 2016;96(5):483-491.

38. Crocchiolo R, Bramanti S, Vai A, et al. Infections after T-replete haploidentical transplantation and high-dose cyclophosphamide as graft-versus-host disease prophylaxis. *Transpl Infect Dis*. 2015;17(2):242-249.

39. Jaiswal SR, Zaman S, Nedunchezhian M, et al. CD56-enriched donor cell infusion after post-transplantation cyclophosphamide for haploidentical transplantation of advanced myeloid malignancies is associated with prompt reconstitution of mature natural killer cells and regulatory T cells with reduced incidence of acute graft versus host disease: A pilot study. *Cytotherapy*. 2017;19(4):531-542.

40. Thakar M, Hari P, Maloney DG, et al. Prophylactic natural killer cell immunotherapy following HLA-haploidentical hematopoietic cell transplantation prevents relapse and improves survival in patients with high-risk hematological malignancies [abstract]. *Blood*. 2016;128:1161.

41. Ciurea SO, Schafer JR, Bassett R, et al. Phase 1 clinical trial using mbIL21 ex-vivo expanded donor-derived NK cells after haploidentical transplantation. *Blood*. 2017;blood-2017-05-785659.

42. Vallera DA, Felices M, McElmurry R, et al. IL15 trispecific killer engagers (TriKE) make natural killer cells specific to CD33+ targets while also inducing persistence, in vivo expansion, and enhanced function. *Clin Cancer Res*. 2016;22(14):3440-3450.

43. Derniame S, Perazzo J, Lee F, et al. Differential effects of mycophenolate mofetil and cyclosporine A on peripheral blood and cord blood natural killer cells activated with interleukin-2. *Cytotherapy*. 2014;16(10):1409-1418.

44. Ohata K, Espinoza JL, Lu X, Kondo Y, Nakao S. Mycophenolic acid inhibits natural killer cell proliferation and cytotoxic function: a possible disadvantage of including mycophenolate mofetil in the graft-versus-host disease prophylaxis regimen. *Biol Blood Marrow Transplant*. 2011;17(2):205-213.

45. Locatelli F, Bauquet A, Palumbo G, Moretta F, Bertaina A. Negative depletion of α/β+ T cells and of CD19+ B lymphocytes: a novel frontier to optimize the effect of innate immunity in HLA-mismatched hematopoietic stem cell transplantation. *Immunol Lett*. 2013;155(1-2):21-23.

46. Di Ianni M, Falzetti F, Carotti A, et al. Tregs prevent GVHD and promote immune reconstitution in HLA-haploidentical transplantation. *Blood*. 2011;117(14):3921-3928.

47. Martelli MF, Di Ianni M, Ruggeri L, et al. HLA-haploidentical transplantation with regulatory and conventional T-cell adoptive immunotherapy prevents acute leukemia relapse. *Blood*. 2014;124(4):638-644.

48. Huang X-J, Zhao X-Y, Liu D-H, Liu K-Y, Xu L-P. Deleterious effects of KIR ligand incompatibility on clinical outcomes in haploidentical hematopoietic stem cell transplantation without in vitro T-cell depletion. *Leukemia*. 2007;21(4):848-851.

49. Armand P, Kim HT, Logan BR, et al. Validation and refinement of the Disease Risk Index for allogeneic stem cell transplantation. *Blood*. 2014;123(23):3664-3671.

50. Sorror ML, Sandmaier BM, Storer BE, et al. Comorbidity and disease status based risk stratification of outcomes among patients with acute myeloid leukemia or myelodysplasia receiving allogeneic hematopoietic cell transplantation. *J Clin Oncol*. 2007;25(27):4246-4254.